HEFAT2014
10th International Conference on Heat Transfer, Fluid Mechanics and Thermodynamics
14 – 16 July 2014
Orlando, Florida

A PARAMETRIC ANALYSIS OF CONVERSION EFFICIENCY OF EARTHEN CHARCOAL MAKING KILN USING A NUMERICAL METHOD

[1]Luwaya Edwin*, [2]Paul Chisale, [3]Francis Yamba, and [4]Mike Malin

*Author for correspondence

[(1,2 & 3)]University of Zambia, School of Engineering
Dept. of Mech. Eng. P.O. Box 32379, Lusaka, Zambia
[4]Concentration, Heat and Momentum Limited, Bakery House, 40 High Street, Wimbledon Village, London, SW19 5AU, UK, E-mail: mrm@cham.co.uk

ABSTRACT

The conversion efficiency of biomass in developing countries in many cases is low resulting in unsustainable use of biomass resources and negative environmental impacts. In the earthen charcoal-making kiln widely used in the developing countries, the conversion efficiency is on average as low as 6 - 10 percent on dry basis. The low conversion efficiency is a source of greenhouse gas causing deforestation around most African cities. However, the earthen charcoal-making kiln has been reported to have potential for improvement of the kiln conversion efficiency. This paper reports on the parametric studies and analysis of the conversion efficiency of the earthen charcoal-making kiln by using a numerical method. To achieve this, a 3-Dimensional transient numerical model of the earthen charcoal-making kiln was used in the CFD (Computational Fluid Dynamics) software code of PHOENICS to simulate the major factors influencing carbonisation processes in the kiln for their effect on the kiln conversion efficiency.

INTRODUCTION

The use of woodfuel which is seemingly affordable by low income urban and rural households is helping wipe out forests in the developing world where meeting energy demand for the growing populations is a daily challenge. In a Sub-Sahara African country like Zambia, woodfuel is the principal source of energy. Deforestation is mainly through the felling of trees for fire wood, charcoal production, expansion and over-exploitation of agricultural land and timber. In Zambia the rate of deforestation from ILUA-generated data was estimated to be 250 000 to 300 000 hectares a year [1, 2].

Many efforts have been done on making thermochemical processes more efficient and economically acceptable. A significant portion of these efforts over the past couple of decades has focused on the development of numerical models of thermochemical reactors (such as gasifiers, pyrolyzers, boilers, combustors, incinerators) that can help to design and analyse the thermochemical process. Due to a combination of increased computer efficacy and advanced numerical techniques, the numerical simulation techniques such as CFD became a reality and offers an effective means of quantifying the physical and chemical process in the biomass thermochemical reactors under various operating conditions within a virtual environment. The resulting accurate simulations can help to optimize the system design and operation and understand the dynamic process inside the reactors [3].

In their current construction and associated field practises, the traditional earthen charcoal kilns consume a lot of wood to produce a relatively small quantity of charcoal thereby contributing immensely to deforestation and global warming through greenhouse gas emissions. They have poor conversion efficiency of 10-15 percent [4]. Generally, studies have shown that any charcoal making kiln with conversion efficiency of 25 percent or less has potential for improvement [5]. That's why this research focused on the parametric studies of the potential and means for raising the efficiency of the earthen charcoal making kiln.

Seifritz [6] stated that approximately 50 percent of the carbon in the wood (mainly the trunk and the thicker branches) can be extracted in the form of charcoal composed of *fixed carbon*, *ash content*, *volatile matter* and *moisture*. In the process of carbonization, considerable amount of carbon is emitted to the air. [7] Compiled past literatures had calculated the average carbon yield of various types of kilns including a laboratory furnace, and reported a figure of 49.9 percent of carbon yield on the average.

This means that half of the total carbon inside wood raw material will be emitted to the air or stored in the form of half-carbonized matter which is easily decomposed (volatile matter). Therefore to raise carbon yield, not only charcoal yield, but also fixed carbon content must be higher.

The traditional earth charcoal kiln has hardly any information on the science and thermodynamics of wood carbonisation processes taking place inside. The matter whether scope does exist for improving the efficiency of the earth charcoal kiln has not received much attention generally. Studies undertaken in Zambia on the earthen charcoal kiln production method assessed the technique from the point of view of the nature of the process efficiency (yield), productivity and cost [8], [9], [10].

Pyrolysis is essentially the thermal decomposition of organic matter under inert atmospheric conditions or in a limited supply of air, leading to the release of volatiles and formation of

char. Pyrolysis in wood is typically initiated at 200°C and lasts till 450-500°C, depending on the species of wood.

Figure 1 shows the main processes involved in pyrolysis of a round wood exposed to a heat flux q_{IN}. Heat conduction into the wood raises the temperature locally, initiating wood drying and subsequent reactions. The reaction front then moves radially inward, leaving a porous char layer behind it. Tar and gas move outwards from this front, finally escaping from the char layer surface. Since pyrolysis is endothermic, this outward flow of volatiles constitutes a cooling convective heat flux which opposes conduction. Other processes occurring during pyrolysis include; secondary reaction of the products passing through the char layer, a build-up of pressure inside the wood to overcome the flow resistance of the porous char, gas phase diffusion of different product species, and shrinkage and/or splitting of the wood [11].

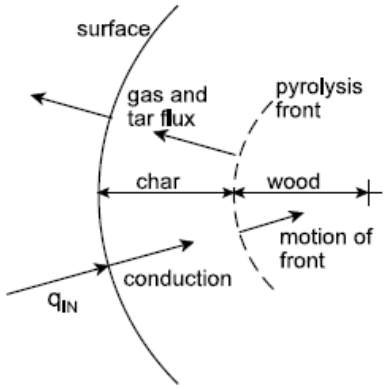

Figure 1 Schematic of Wood Pyrolysis.

The overall process of pyrolysis of wood is believed to proceed as follows: At around 160°C the removal of all moisture (dehydration) is complete. Over the temperature range 200°C to 280°C, all the hemicellulose decomposes, yielding predominantly volatile products such as carbon dioxide, carbon monoxide and condensable vapours. From 280°C to 500°C the decomposition of cellulose picks up and reaches a peak around 320°C. The products are again predominantly volatiles. The decomposition rate of lignin increases rapidly at temperatures beyond 320°C. This is accompanied by a comparatively rapid increase in the carbon content of the char residual solid material [12]. A comprehensive review of the basic phenomena of pyrolysis can be found elsewhere [13].

NUMERICAL METHOD

The thermochemical and diffusion processes within the logs were represented within the kiln domain by the general transport equations of continuity, momentum, energy, gas-phase species, solid-phase species, and the state equation of system. The supporting physical models used were the interphase momentum transfer, interphase heat transfer, pyrolysis, wood drying and the radiative-heat-transfer models.

It was the purpose of the developed models to simulate the densities, temperature fields, species concentrations e.t.c within the charcoal kiln domain for different input values of the major factors likely to influence kiln conversion efficiency.

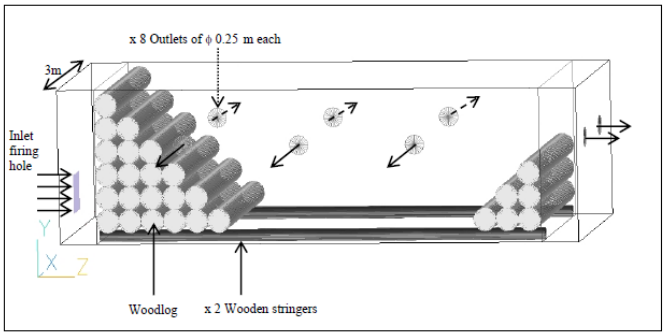

Figure 2 Kiln physical domain

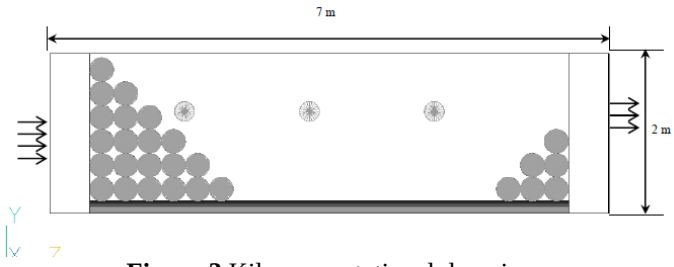

Figure 3 Kiln computational domain

The finite volume method (FVM) and iterative method together with convergence acceleration approach were applied to solve the governing partial differential equations system in integral forms of a series of physical models for wood pyrolysis using Intel PHOENICS 2009 solver.

The charcoal kiln domain was modelled using a cartesian coordinate system. Its physical and computational domain (Figures 2 and 3) was divided into discrete control volumes (3D cells or mesh) using rectangular-type grids, Figures 4. This mesh has cells having a hexahedral-shape element with eight-nodal corner points in three-dimensions. This structured grid generation is simple and enables the user to adaptively refine the mesh in areas that contain complex flow structures, such as bends, regions of recirculation zones, inlets and outlets for the domain.

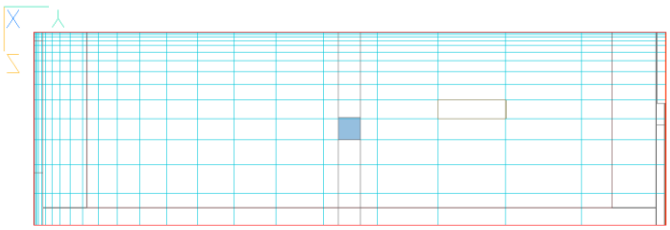

Figure 4 The grid mesh

It was found that for the developed models, mesh–independence of the various variables solutions was obtained with a 9 x 25 x 17 mesh in the x- *y*- and *z*-coordinates. When the number of iterations was increased by 50 percent, less than 3 percent difference in the calculated variables solutions was present. All subsequent simulation work was performed with this mesh size.

Initial Conditions

The iterative procedure used requires initialisation of all the discrete values of the flow properties and other transport parameters of interest before computing the solution. The initial conditions for the transient simulation are summarised below:

Solid phase

Wood temperature = 20°C.
Wood moisture content, Y_{w0} = 0.15.
Mass fraction of raw wood that is volatile matter, Y_{vs0} = 0.15.
Mass fraction of raw wood, = 0.85.
Wood density, ρ_{s0} = 600 kg/m^3.

Gas phase

The initial relative humidity of the air, R_h = 14.0%.
Gas temperature, T_{g0} = 20°C.
Gas velocity = 0 m/s.

Ignition source

For simplicity, the firing of the kiln was achieved artificially by introducing a heat source into the airstream upstream of the fixed bed of woodlogs as follows:

- 0 to 14 hours - linear from 0.2MW to 0.7MW
- 14hours and onwards- uniform at 0.7MW.

This heat source is uniformly distributed over the kiln inlet area of W_k=1.5m by L_k=10m initial size opening.

Inlet Boundary Conditions

The air stream approaching the kiln was assigned the following conditions:

Air relative humidity of the air, = 14.0%.
Air temperature = 20°C.
Air inlet velocity = 5m/s.

Outlet Boundary Conditions

The outlet boundary is initially located downstream of the kiln, and a fixed pressure condition was used at this boundary. In the later final models the outlets were located on the sides and end of kiln all of similar size and positioned at kiln mid height. Refer to kiln geometry diagram in Figure 3.

For the numerical solution, the balance equations were solved in a finite-volume formulation. The finite volume equations (FVE's) are obtained by integrating the differential equation over the cell volume to construct the algebraic equation system for discrete unknowns.

The prevailing wind direction in this model represents the external environment surrounding the kiln. Simulation of the effects of the prevailing wind direction are taken care of by a WIND object embedded in the CFD software used.

FLOW PROPERTIES WITHIN KILN

Presented here are the flow properties results from the numerical simulations of the model using optimised factors influencing the kiln conversion efficiency.

SPATIAL DISTRIBUTION OF CARBONISATION VARIABLES

(i) Pressure and Velocity Distribution

The pressure distribution shown in Figure 5 was taken along the centreline of the kiln model. The pressure is uniformly distributed in the kiln within range of 0.244-0.520 Pa. The kiln is fired by an external source of energy. At the firing point of the kiln the pressure is intense (2.45 to 3.00 Pa) due the combustion process taking place to fire the kiln.

Source: Model results.

Figure 5 Pressure contours along the kiln length

The case of model velocity vector plots, depicted in Figure 6, is for a kiln fired along the prevailing wind direction. The velocity distribution in the kiln is fairly uniform between 0.837 to 1.247 m/s. This velocity is slightly lower than the average 2.3 m/s measured in the field. The logs resistance in the kiln reduce this superficial velocity of 2.3 m/s measured in the field.

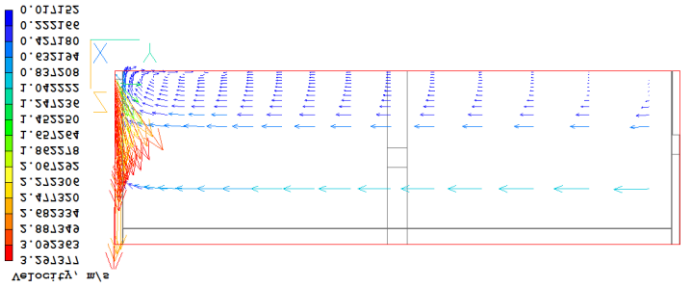

(a)

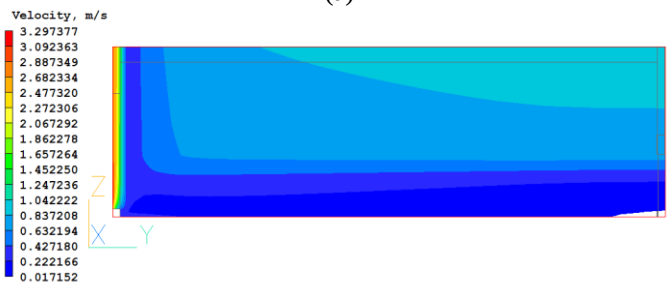

Source: Model results.

(b)

Figure 6 Velocity distributions along kiln length (a) vectors and (b) contours

(ii) Temperature Distribution

Pyrolysis at lower kiln temperatures favours the production of charcoal whereas at higher temperatures results in

the fission, dehydration, disproportionation, decarboxylation and decarbonylation reactions, which favours gas production. The temperature distribution shown in Figure 7 model results is at the end of the 16.75 days of carbonisation period simulated. The peak temperature in the simulation results was 400 °C, which matches the carbonisation temperature requirements for maximised charcoal production.

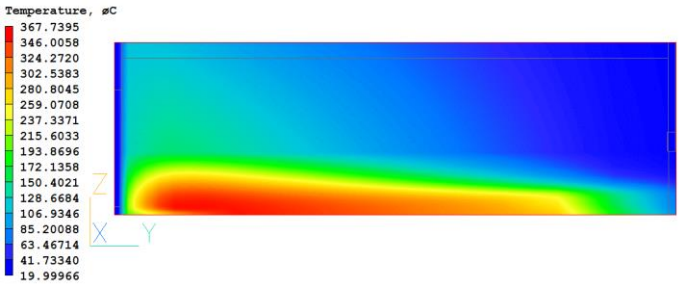

Source: Model results.

Figure 7 Temperature distributions along kiln length

There is better heat intensity and distribution at the kiln lower left region near the entrance in Figure 5.17. This enhanced the low velocity and recirculation in this region as observed in Figure 5.16 (a) and (b) for better carbonisation.

(iii) Radiation Energy Distribution

Model results in Figure 8 (a)-(c) are contour plots of radiation energy in kW/m^3 in the X-, Y- and Z-directions in the kiln. The radiation energy in the X-direction is uniform at 284 kW/m^3. The radiation energy in the Y-direction is at 264 kW/m^3. The Z-direction radiation energy is at an average 2401.43 kW/m^3. The radiation energy is high where the kiln temperature is high in the Y-direction. The intense radiation energy results in higher heat of pyrolysis and better carbonisation for higher charcoal yield.

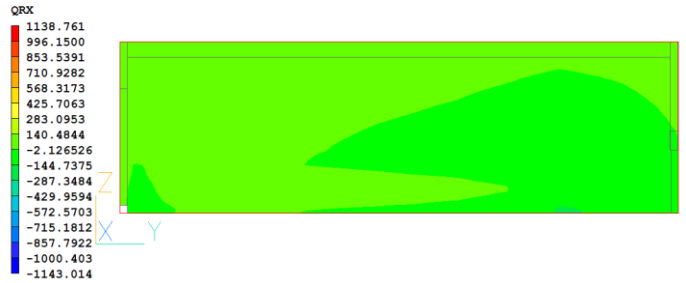

(a)

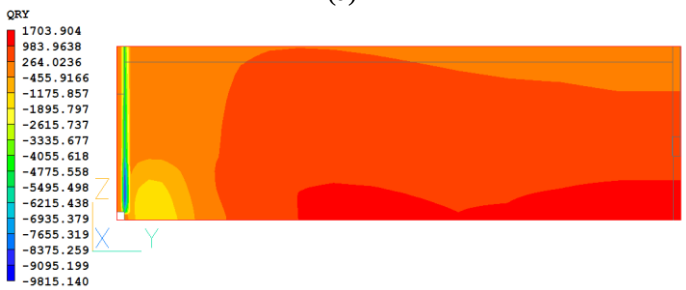

(b)

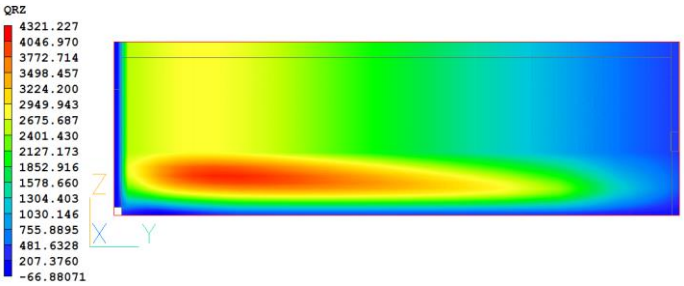

(c)

Source: Model results.

Figure 8: Radiation energy distribution along kiln length (a) X-direction (b) Y-direction and (c) Z-direction

(iv) Gas Phase Distribution

In Figure 9 (a) there is low air concentration in the first half of the kiln as it is consumed for combustion initiation and carbonisation in the kiln. The second half of the kiln in (a) has high concentration of air as carbonisation has not taken place in this second half of the kiln.

In Figure 9 (b) there is low concentration of water vapour in the first half of the kiln where the wood has been dried from intense heat from the kiln firing combustion. The water vapour concentration is high in the second half of the kiln where the wood is yet to be dried prior to carbonisation.

In Figure 9 (c) the concentration of volatile gases is high in the first half of the kiln where carbonisation has taken place while the second half of the kiln has low concentration of volatile gases since carbonisation is yet to take place.

(a)

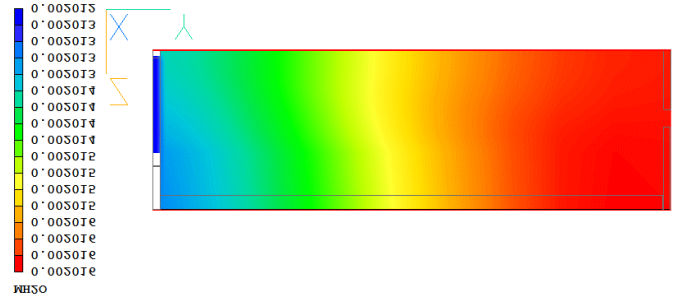

(b)

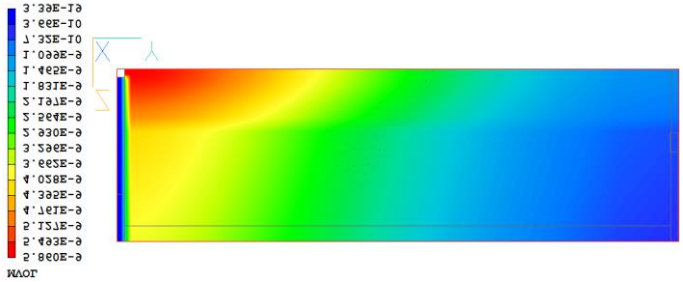

(c)

Source: Model results.

Figure 9 Gaseous phase distribution along kiln length (a) air (b) water vapour and (c) volatiles.

(v) Solid Phase Distribution

The solid phase is made up of the *raw wood* logs, *water* (moisture) in the logs and the *charcoal* produced. In Figure 10 (a) the water moisture fraction is low in the first half of the kiln as the wood has been converted to charcoal but the moisture fraction is high in the last half of the kiln where carbonisation has yet to take place and raw wood is abundant.

In Figure 10 (b) the fraction of raw wood is low in the first half of the kiln where it has been carbonised to charcoal, but the second half of the kiln has high fraction of raw wood since carbonisation is yet to take place.

In Figure 10 (c) three quarters of the kiln has a high fraction of charcoal fraction. This is expected as the wood is carbonised, the water fraction decreases and so is the fraction of raw wood, which is being converted to charcoal hence the charcoal fraction increases instead.

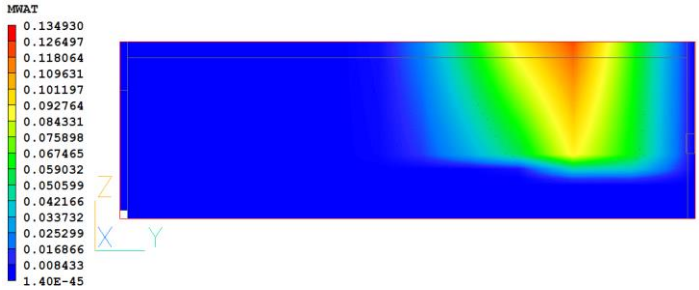

(a)

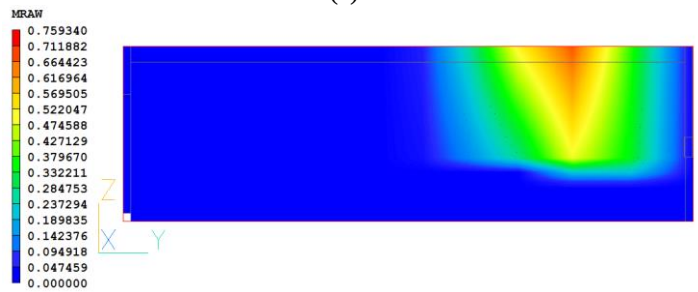

(b)

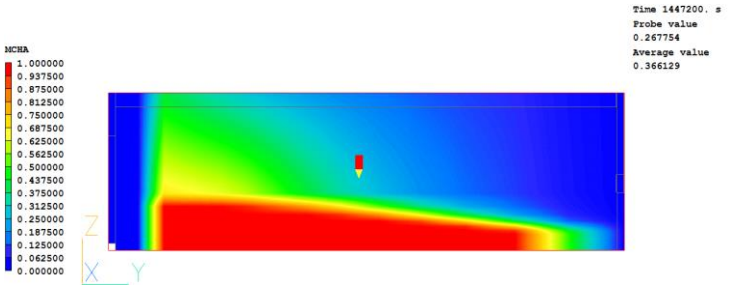

(c)

Source: Model results.

Figure 10: Solid phase distribution along kiln length (a) moisture (b) raw wood and (c) charcoal

TEMPORAL EVOLUTIONS OF CARBONISATION VARIABLES

(i) Wood Density and Temperature

Figure 11 model results depicts that as the wood temperature increases, from ambient temperature of 20°C to about 420°C in 4 days, the wood density drops from initial 350 kg/m^3 to about 275 kg/m^3. At 420°C the carbonisation process ends with production of charcoal. During pyrolysis of the wood there is a rise in temperature and evolution of volatile gases and water vapour leading to significant loss of mass and drop in density. The resulting wood volume shrinkage is insignificant to warrant an increase in the wood density. The shape of charcoal pieces observed in the field showed that shrinking of wood takes place to a small extent.

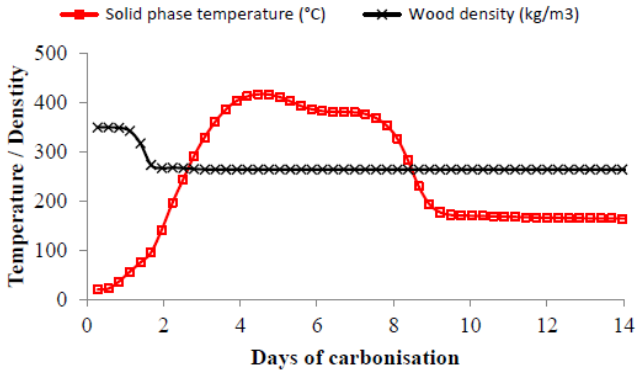

Source: Model results.

Figure 11 Temporal distribution of wood density and kiln temperature

(ii) Drying, and Pyrolysis rates per unit volume

Figure 12 model results depicts that a day and half after firing the kiln, the drying and pyrolysis processes commence with their rates increasing rapidly to a peak of 0.0045 kg/m^{3}s and drops to zero rate on the second day of carbonisation. Field observations showed that drying and pyrolysis rates are very crucial in the carbonization process as they mostly depend on the kiln management and the initial wood logs preparations especially the degree of drying.

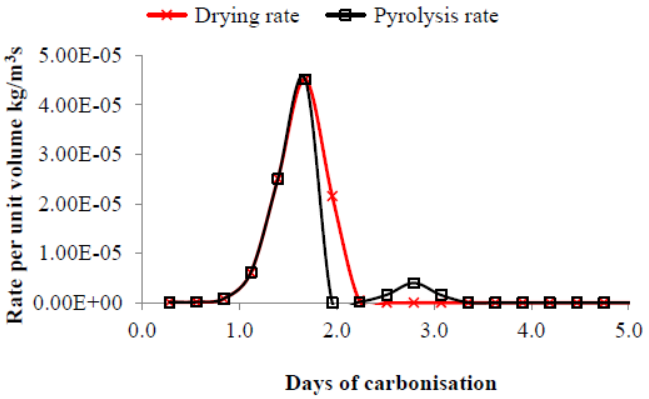

Source: Model results.

Figure 12 Temporal distributions of drying and pyrolysis rates

(iii) Solid and gas phase temperatures

It is observed in Figure 13 model results that the wood temperature increases steadily from ambient of 20°C to about 420°C during the first 4 days. The gases temperature follows the same pattern as the solid phase temperature. On a kiln in the field, it was observed that as the carbonization temperature increased in the kiln, very hot gases were evolving from the kiln wall perforations at very high temperature.

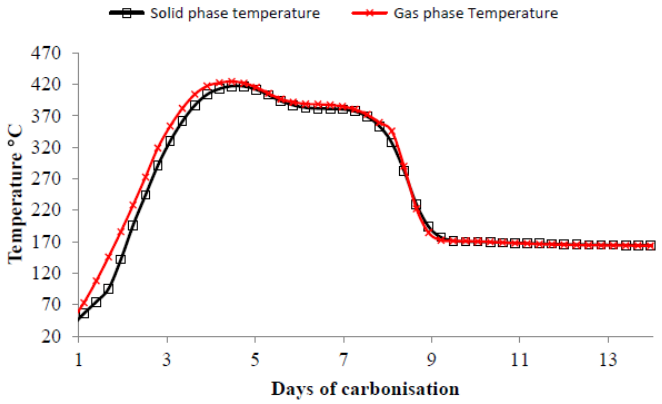

Source: Model results.

Figure 13 Temporal distributions of solid and gas phase temperatures

(iv) Solid Phase Mass Fractions

In the Figure 14 model results it is observed that 24 hours after kiln is fired, drying, and carbonisation starts in the kiln. After 48 hours the moisture mass fraction decreases to zero. The raw wood mass fraction decreases to zero in 72 hours after kiln firing. Charcoal starts forming 24 hours after firing kiln and its mass fraction reaches one after 72 hours and remains constant for the rest of the carbonization process. In an actual kiln there are usually varying proportions of charcoal, and uncarbonised wood brands especially towards the end of the kiln. The mass fractions of these components depend on the kiln management and wood preparation prior to carbonization.

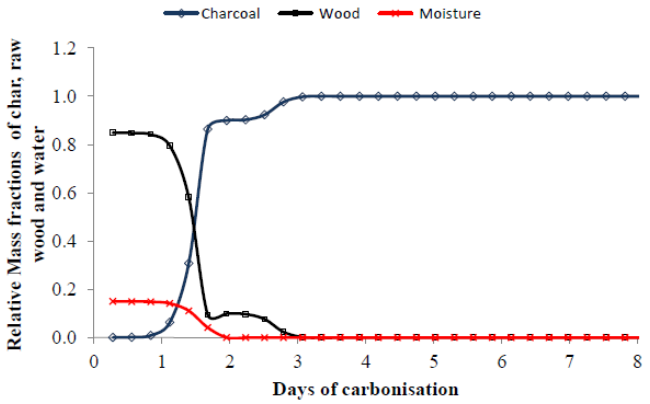

Source: Model results.

Figure 14 Temporal distributions of solid phase mass fractions

Optimisation of the Kiln

The optimised variables and fixed factors relative conversion efficiencies were used to calculate the optimal kiln conversion efficiency and charcoal yield. The relative conversion efficiency and relative charcoal mass fraction are optimised parameters obtained by simulating only one factor of influence at a time.

TRENDS AND RESULTS

All the model simulations were carried out in a standard kiln of dimensions 2 m high x 3 m wide x 7 m long.

Effect of properties of wood

Density of wood

Figure 15 depicts the model results of the plot of the change of density of wood and the resulting relative charcoal fraction. Changing the density from 350 kg/m^3 (softwoods) to 1250 kg/m^3 (hard woods) did not change the relative charcoal fraction of 0.32 at all. This agrees with S.H Hibajene's observations in the field that changing the wood species did not change the charcoal yield [14].

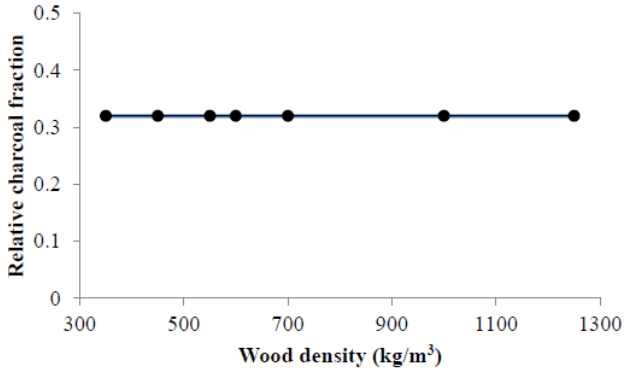

Source: Model results.

Figure 15 Relative charcoal fraction versus wood density in an earth kiln

Diameter of wood log

In Figure 16 from the model results it can be observed that both cross loaded and longitudinal loaded kilns have their relative charcoal fractions reduced as the diameter of the logs increase. The model results in Figure 9 also show that the longitudinally loaded kiln performs better than the cross loaded kiln.

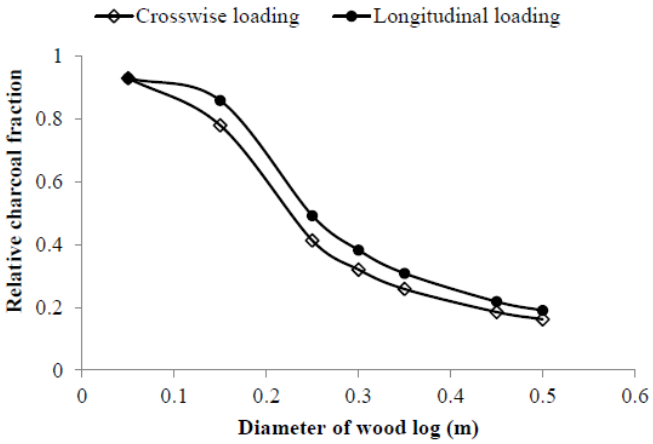

Source: Model results.

Figure 16 Relative charcoal fraction versus diameter of wood log

Moisture Content of Wood logs

The research model results in Figure 17 show that as the moisture content in the wood was reduced from 35 percent to 12 percent the relative charcoal fraction increased from 0.272 to 0.577 respectively.

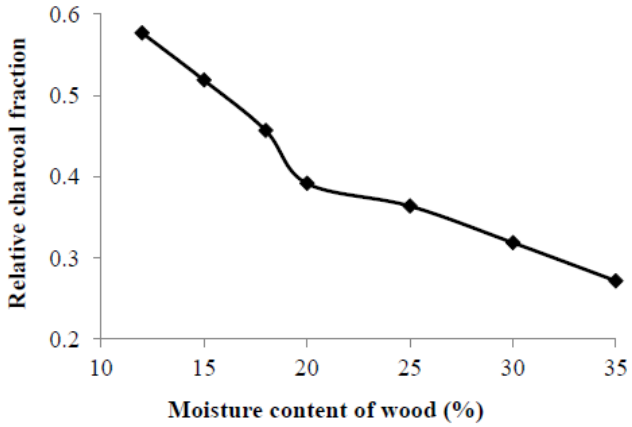

Source: Model results.

Figure 17 Relative charcoal fraction versus moisture content of wood

Effect of Kiln Design

The model results in Figure 18 show that for both crosswise and longitudinal loaded kilns, the relative charcoal fraction was extremely poor (0,032) for a 1.5 m wide kiln but 0.928 for the 2.0 m wide kiln. For kiln widths of 2.5 m and above, the relative charcoal fraction for the crosswise loaded kiln kept decreasing as the kiln width was increased while for the longitudinally loaded kiln the relative charcoal fraction did not change with increasing kiln width.

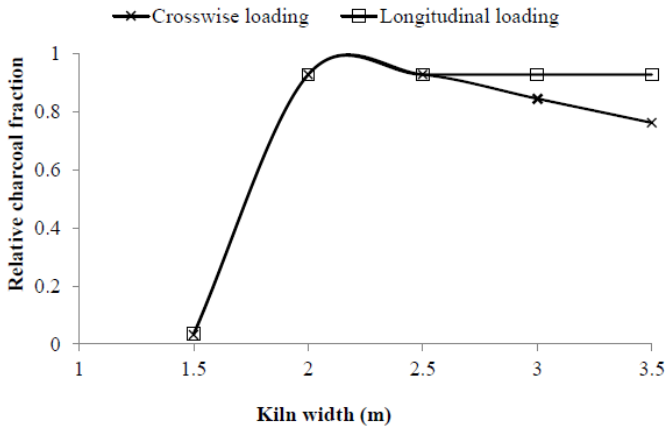

Source: Model results.

Figure 18 Relative charcoal fraction versus kiln width.

Length of Kiln

Based on model results, Figure 19 shows the relative charcoal fraction variance with kiln length for both cross loaded and longitudinal loaded kilns. The relative charcoal fraction ranges from 0.85 to 0.95 for the two types of wood loading. Both types of loading were tested for kiln lengths from 3.5 m to 21.0 m. For the cross loaded kiln the relative charcoal fraction averaged 0.871 over the kiln length range. The longitudinal loaded kiln relative charcoal fraction averaged 0.940 over the kiln length.

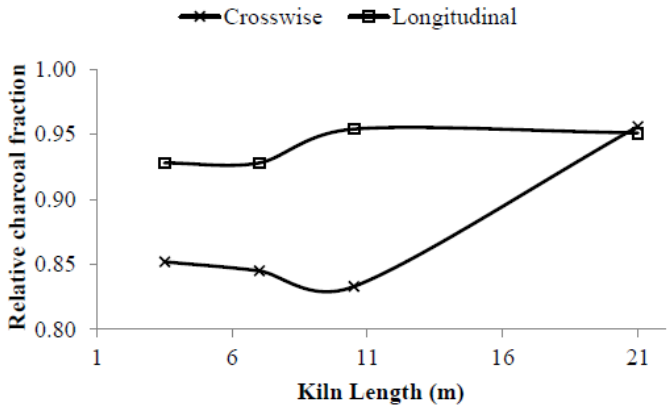

Source: Model results.

Figure 19 Relative charcoal fraction versus kiln length.

Thickness of Insulating Wall

The numerical results from the model in Figure 20 show that the relative charcoal fraction falls from some maximum value and falls as the insulation wall thickness is increased for both cross and longitudinal loaded kilns. For the cross loaded kiln the relative charcoal fraction decreases from 0.482 with wall thickness of 0.1 m to 0.229 with wall thickness of 0.6 m. In the case of longitudinally loaded kiln, the relative charcoal fraction falls from 0.667 at 0.1 m thick insulation wall to 0.192 with insulation wall thickness of 0.6 m.

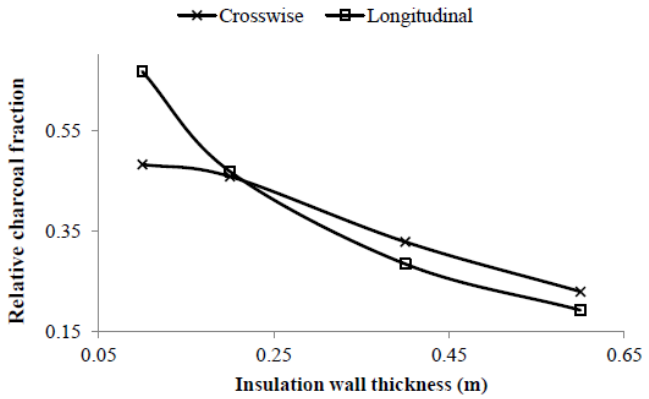

Source: Model results.

Figure 20 Relative charcoal fraction versus insulation wall

Log Diameter Size Effect

Figure 16 earlier on shows the model results for both crosswise and longitudinal type of loading, the relative charcoal fraction decreases as the diameter of the wood log increases from 0.1 m to 0.50 m. The results also show that small diameter logs are best used in longitudinally loaded kilns.

Uniform diameter log distribution effect

Two kilns, one crosswise and the other longitudinal loaded, were simulated. Each kiln was stacked with uniform diameter wood logs *(0.250 m)*. Model results in Figure 15 show that the longitudinally loaded kiln has a higher relative charcoal fraction (0.491) than the crosswise loaded kiln (0.412).

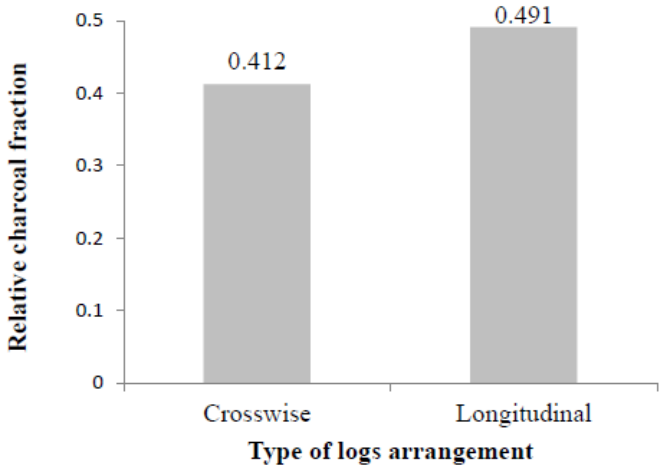

Source: Model results.

Figure 21 Relative **c**harcoal fraction versus logs arrangement *(uniform diameter)*.

Non- uniform diameter log distribution effect

Model results in Figure 21 show that the longitudinally loaded kiln had a higher relative charcoal fraction (0.928) than the cross loaded kiln (0.845).

From the model results of Figure 22 it can be observed that:

(i) For the ***crosswise*** type of loading the use of non-uniform diameter wood logs has higher relative charcoal fraction (0.845) than the use of uniform diameter wood logs (0.412) even though the uniform diameter woodlogs were of the medium diameter category.

(i) In the ***longitudinal*** type of loading higher relative charcoal fraction is obtained (0.928) when use is made of non-uniform diameter wood logs than when uniform diameter wood logs are used (0.491).

(ii) Overall the longitudinal type of wood log arrangement preferably stacked with non-uniform diameter logs in the medium diameter category has better charcoal yield.

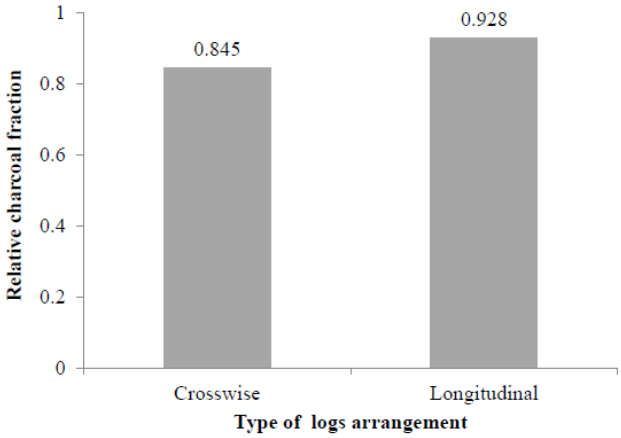

Source: Model results.

Figure 22 Relative **c**harcoal fraction versus logs arrangement *(non-uniform diameter)*.

The Figure 23 shows model results for the overall comparison of the ***crosswise*** loaded kiln with the ***longitudinal*** loaded kiln in terms of use of ***uniform diameter*** logs and ***non-uniform diameter*** logs.

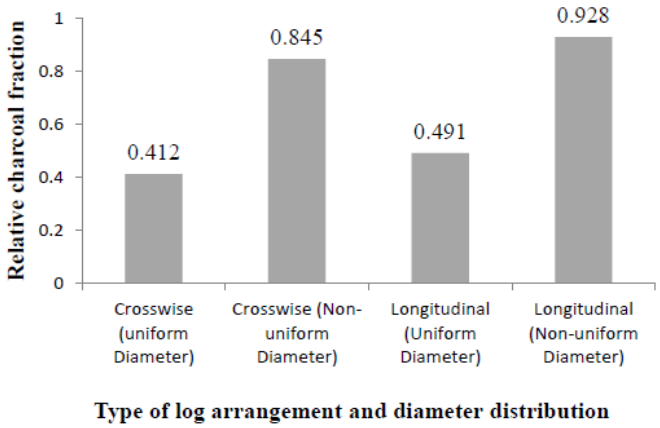

Source: Model results.

Figure 23 Relative charcoal fraction versus logs arrangement and diameter distribution

Effect of Direction of Prevailing Wind to Direction of Carbonisation

The model results in Figure 24 show the relative charcoal fraction for two crosswise loaded kilns in prevailing wind streams of opposite directions. The first kiln has its carbonisation direction against the direction of the prevailing wind and resulted in a relative charcoal fraction of 0.369. The second kiln's direction of carbonisation was along the prevailing wind direction and resulted into a relative charcoal fraction of 0.642.

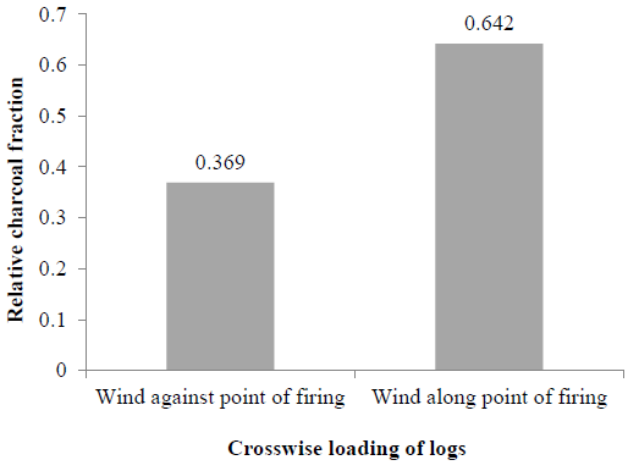

Source: Model results.

Figure 24 Relative **c**harcoal fraction versus wind direction *(Crosswise).*

Effect of prevailing wind direction in longitudinal loaded kiln

The model results in Figure 25 show the relative charcoal fraction for two longitudinally loaded kilns in prevailing wind streams of opposite directions. The first kiln has its carbonisation direction against the direction of the prevailing wind and resulted in a relative charcoal fraction of 0.632. The second kiln's direction of carbonisation was along the prevailing wind direction resulting into a relative charcoal fraction of 0.452.

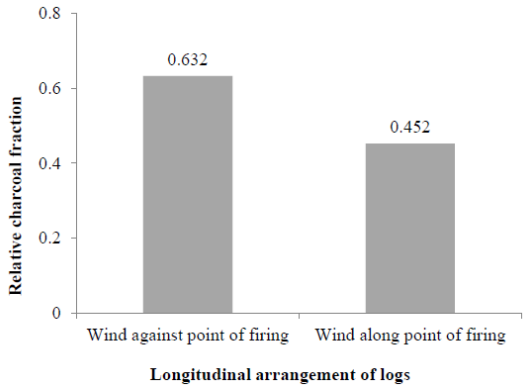

Source: Model results.

Figure 25 Relative **c**harcoal fraction versus wind direction *(Longitudinal)*

CONVERSION EFFICIENCY

The efficiency of a kiln is defined as *the mass of charcoal that a producer obtains from a kiln expressed as a percentage of the mass of wood the producer initially charged into the kiln*. Strictly speaking, this is the **recovery efficiency**. The **conversion efficiency** includes even the charcoal fines (rejects) that may not be packaged for sale due to their small size [15].

Several major factors likely to influence the conversion efficiency in the charcoal kiln were identified and parametrically studied in the numerical model. These factors were:

(i) density of the wood.
(ii) moisture content of the wood.
(iii) diameter of the wood logs.
(iv) weight distribution and arrangements of the wood logs.
(v) size of the kiln in terms of width and length.
(vi) thickness of earth insulating wall.
(vii) direction of carbonisation in relation to prevailing wind direction.

Conversion efficiency for crosswise loaded kiln

E_{ck} = 0.88 x 0.928 x 0.845 x 0.642 x 0.577 x 0.482 x 100 =
12.36 percent

Conversion efficiency for Longitudinal loaded kiln

E_{ck} = 0.883 x 0.928 x 0.928 x 0.632 x 0.577 x 0.667 x 100 =
18.50 percent

CHARCOAL YIELD OF KILN

Usually, efficiency of charcoal production is indicated by charcoal yield. Figure 26 shows the carbon in wood material and pure carbon in charcoal [16].

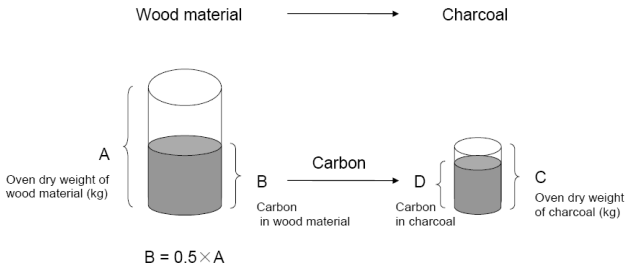

Figure 26 Carbon in wood material and pure carbon in charcoal**.**

To calculate the charcoal yield of the kiln, Equation 3.41 was used. In this equation the ratio $\frac{C}{A}$ represents the conversion efficiency E_{ck} as determined in section 5.8.2. The moisture content of 12 percent being the optimum was used in the equation

Charcoal yield for crosswise loaded kiln

$$\text{Charcoal yield}\,(\%) = \frac{C}{A} \text{ x } \frac{100}{100 - \text{Moisture content}\,(\%)}$$

$$= 12.36 \text{ x } \frac{100}{100 - 12} = \mathbf{14.05\,percent}$$

Charcoal yield for Longitudinal loaded kiln

$$\text{Charcoal yield}\,(\%) = \frac{C}{A} \text{ x } \frac{100}{100 - \text{Moisture content}\,(\%)}$$

$$= 18.50 \text{ x } \frac{100}{100 - 12} = \mathbf{21.02\,percent}$$

These model results are reportedly an improvement on the conversion efficiency and charcoal yield of a traditional earth charcoal making kiln which are reported as having a conversion efficiency of as low as 5 - 10 percent. Hibajene's field results reported an improvement of charcoal yield of not more than 25 percent for each of the factors investigated for both the crosswise and longitudinal loaded kilns.

CONCLUSION

The results showed that seven major factors have some influence on the carbonisation process and the kiln conversion efficiency. The favourable factors are the low ***moisture content*** of the wood, smaller ***diameter*** logs, wood ***weight distribution***, w***ood arrangement***, ***kiln width, kilns length, insulation thickness layer*** and the ***prevailing wind direction*** in relation to carbonisation direction.

From the numerical model results, the optimised overall *conversion efficiency* and *charcoal yield* for the crosswise loaded kiln were found to be 12.36 percent and 14.05 percent respectively, while for the longitudinally loaded kiln these figures were 18.50 percent and 21.02 percent respectively. These figures match well with those reported in literature and empirical observations of earthen charcoal making kilns

REFERENCES

1. ILUA, *Integrated Land Use Assessment 2005 - 2008*, Forestry.Department and Department, Editors. 2010: Lusaka, Zambia.
2. Zambia, *Integrated Land Use Assessment (ILUA)*, Z. Forestry, Editor. 2005-2008: Lusaka.
3. Wang, Y. and L. Yan, *CFD Studies on Biomass Thermochemical Conversion* International Journal of Heat and Mass Transfer Molecular Sciences ISSN 1422-0067 2008. **9**( ): p. 1108-1130.
4. Foley, G., *Charcoal Making in Developing Countries, Technical Report No. 5. Earthscan* 1986, International Institute for Environment and Development: London.
5. FAO, *Industrial Charcoal Making, Paper 63*. 1985, FAO Forestry Department: Rome.
6. Seifritz, W., *Should we store carbon in charcoal?* . Int. J. Hydrogen Energy, 1993. **Vol.18**(No.5): p. 405-407.
7. Glazer, B., Lehmann, J. , and Zech, W., *Ameliorating physical and chemical properties of highly weathered soils in the tropics with charcoal – a review*, in *Biol Fertil Soils.* 2002. p. 219-230.
8. Ranta, J. and Makunka, J., *Charcoal from Indigeneous and Exotic Species in Zambia*, Forest Department, Division of Forest Products Research, Editor. 1986.
9. World Bank/ESMAP, *Zambia Household Energy Strateg Report*. 1990: Washington D.C.
10. Chidumayo, E., .*Woody Biomass Structure and Utilization for Charcoal production in a Zambian Miombo Woodland.* Bioresource Technology, 1991a. **37**: p. 43-52.
11. Tuck, A.R.C. and Hallett, W.L.H., *Modelling of Particle Pyrolysis in a Packed Bed Combustor*. 2005, University of Ottawa, Depts. of Chemical and Mechanical Engineering: Ottawa, Ontario.
12. Roberts, A.F., *Problems Associated with the Theoretical Analysis of the Burning of Wood*, in *16th Int. Symposium on Combusion*. 1971, The Combustion Institute: Pitts. p. 893-903.
13. Zaror, C.A. and D.L. Pyle. *The Pyrolysis of Biomass: A General Review*. in *Proc. Indian Acad. Sci. (Eng. Sci)*. 1982. India.
14. Hibajene, S.H., *Assessment of Earth Kiln Charcoal Production Technology*. 1994, Department of Energy,, Ministry of Energy and Water Development: Lusaka.
15. Hibajene, S.H. and Kalumiana, O.S., *Manual for Charcoal Production in Earth Kilns in Zambia.* , Department of Energy, Ministry of Energy and Water Development, Editor. 2003: Lusaka, Zambia.
16. Gustan, P., *Charcoal production for carbon sequestration. Demonstration Study on Carbon Fixing Forest Management in Indonesia*. 2004, Forest Products Technology Research and Development Center and Japan International Cooperation Agency.